

# ADVANCED FIRST-PRINCIPLE STUDY OF $\text{AgGaTe}_2$ AND $\text{AgInTe}_2$ CHALCOPYRITE SEMICONDUCTORS: STRUCTURAL, ELECTRONIC, AND OPTICAL PROPERTIES VIA FPLAPW WITHIN WIEN2K

Abdelghani Koubil<sup>1</sup>, Mohamed Khettal<sup>1</sup>,  Yousra Megdoud<sup>1</sup>,  Mosbah Laouamer<sup>2</sup>,  
 Yamina Benkrima<sup>3\*</sup>, Latifa Tairi<sup>4</sup>,  Redha Meneceur<sup>2</sup>

<sup>1</sup>Institute of Sciences, University Center of Tipaza, Algeria

<sup>2</sup>UDERZA Unit, Faculty of Technology, University of El-Oued, 3900 Algeria

<sup>3</sup>Ecole Normale Supérieure de Ouargla 3000 Algeria

<sup>4</sup>Research Center in Industrial Technologies CRTI, P.O. Box 64, Cheraga, 1, 6014 Algiers, Algeria

\*Corresponding Author Email: [b-amina1@hotmail.fr](mailto:b-amina1@hotmail.fr)

Received July 15, 2025; revised October 2, 2025; accepted October 3, 2025

In this paper, we present a detailed theoretical exploration of the ternary chalcopyrite semiconductors  $\text{AgGaTe}_2$  and  $\text{AgInTe}_2$  using first-principles calculations grounded in Density Functional Theory (DFT). The simulations are carried out within the Full-Potential Linearized Augmented Plane Wave (FPLAPW) formalism as implemented in the WIEN2k computational package. Structural properties are optimized using the WC-GGA exchange–correlation functional, whereas the electronic and optical responses are refined through the modified Becke–Johnson (mBJ) potential, known for its improved bandgap estimation accuracy. The study involves a thorough evaluation of the electronic band structures and various optical parameters, including the complex dielectric function, absorption coefficient, refractive index, energy-loss function, and reflectivity. The findings reveal that both materials possess direct bandgaps that lie within the optimal range for solar cell absorption. Additionally, these compounds show strong light absorption in the visible and near-infrared regions, high refractive indices, and marked interband transitions. Such features highlight their suitability for photovoltaic technologies, especially in thin-film configurations where enhanced light capture and carrier generation are critical. Moreover, the observed optical and electronic properties also suggest possible utilization in infrared detection and nonlinear optoelectronic systems. Overall, the results contribute valuable theoretical insight into the optoelectronic characteristics of silver-based telluride chalcopyrites, reinforcing their potential as environmentally friendly and efficient materials for future solar energy solutions.

**Keywords:** FPLAPW; Density Functional Theory; Modified Becke–Johnson; Electronic structure; Optical analysis

**PACS:** 73.20.At, 78.20.Ci

## 1. INTRODUCTION

Ternary I–III–VI<sub>2</sub> chalcogenide semiconductors, notably  $\text{AgGaTe}_2$  and  $\text{AgInTe}_2$ , have garnered substantial attention from the scientific community owing to their remarkable structural and physicochemical characteristics.

These compounds are part of a wider family of tellurium-rich materials that adopt a crystal structure based on the chalcopyrite prototype [2]. Their combination of adaptable crystal geometry, adjustable bandgap energy, and superior optical activity across the visible and infrared spectra renders them highly suitable for innovative energy-related and optoelectronic applications [3–8].

$\text{AgGaTe}_2$  and  $\text{AgInTe}_2$  crystallize in a chalcopyrite-type tetragonal lattice (space group I-42d, No. 122) [9], derived from the zincblende structure through an ordered arrangement of cations. This structural configuration exhibits a distinct distribution of atoms at cationic and anionic positions, leading to anisotropic electronic properties and notable dielectric responses.

Thanks to their relatively narrow and direct bandgaps, both materials are highly suited for use in thin-film solar cells, infrared photodetectors, thermoelectric converters, and nonlinear optical applications [10–15]. Furthermore, their optoelectronic characteristics can be engineered through compositional modifications or lattice strain, enhancing their adaptability for tailored device integration.

Despite their promising functionalities, rigorous theoretical investigations, particularly those employing accurate *ab initio* techniques, remain limited. Among such methods, the Full-Potential Linearized Augmented Plane Wave (FPLAPW) approach [16] is widely regarded for its high precision in solving the Kohn–Sham equations within the Density Functional Theory (DFT) framework [17], especially for systems exhibiting structural anisotropy or complex bonding environments.

In this study, we utilize the WIEN2k computational platform [18], a well-established implementation of the FPLAPW formalism, to explore the structural, electronic, and optical properties of  $\text{AgGaTe}_2$  and  $\text{AgInTe}_2$ . Geometry optimization is conducted using the Wu–Cohen Generalized Gradient Approximation (WC-GGA), while the electronic and optical responses are computed via the modified Becke–Johnson (mBJ) potential [19], which offers superior bandgap accuracy compared to traditional GGA or LDA functionals.

The objective is to provide a thorough characterization of these compounds, including their:

- electronic band structures and bandgap nature (direct vs. indirect),
- and Optical parameters, such as the dielectric function, absorption coefficient, refractive index, and reflectivity [15].

The findings provide valuable theoretical insights for optimizing Ag-based chalcopyrite semiconductors in energy harvesting and optoelectronic applications, while supporting their development as efficient and sustainable materials for next-generation technologies.

## 2. COMPUTATIONAL METHODOLOGY

All computational analyses in this study were conducted using the WIEN2k package [18], which implements the Full-Potential Linearized Augmented Plane Wave (FPLAPW) method [16] recognized as one of the most precise first-principles techniques for solving the Kohn–Sham equations of Density Functional Theory (DFT) [17]. This approach is particularly effective for handling materials with strongly localized or correlated electrons, such as those containing transition metals or heavy elements.

For structural relaxation and total energy determination, we employed the Generalized Gradient Approximation (GGA) with the Perdew–Burke–Ernzerhof (PBE) exchange correlation functional [20]. To enhance the accuracy of the computed electronic bandgaps and optical properties, we adopted the modified Becke Johnson (mBJ) potential, which is known to yield bandgap estimates that align more closely with experimental results than those obtained using standard GGA or LDA methods.

Given the presence of the heavy tellurium (Te) atom ( $Z = 52$ ), spin–orbit coupling (SOC) effects were explicitly considered, as they significantly influence the electronic states near the valence band maximum. Computational parameters were carefully selected to ensure numerical accuracy and convergence: the plane-wave cutoff parameter  $RK_{\text{max}}$  was set to 8.0, and the Brillouin zone was sampled with a  $12 \times 12 \times 12$  Monkhorst Pack  $k$ -point mesh.

Muffin-tin radii ( $R_{\text{MT}}$ ) were assigned as follows: 2.5 atomic units (a.u.) for Ag, 2.3 a.u. for Ge or In, and 2.4 a.u. for Te, ensuring there was no overlap between atomic spheres. Self-consistent field (SCF) cycles were considered converged when the total energy difference between iterations was less than  $10^{-5}$  Ry, and the charge convergence threshold was set to  $10^{-4}$  Ry.

## 3. RESULTS AND INTERPRETATION

### 3.1. Structural Optimization

The structural optimization of the ternary chalcopyrite compounds  $\text{AgInTe}_2$  and  $\text{AgGaTe}_2$  offers crucial insights into their crystal stability, atomic-scale arrangement, and the structural parameters that influence their physical behavior. Both compounds crystallize in the tetragonal chalcopyrite structure with space group I-42d, [9] which can be regarded as a derivative of the cubic zinc blende structure. This configuration arises through the ordered substitution of Group III elements (In or Ga) and the resulting doubling of the unit cell along the  $c$ -axis. The ordered arrangement of cations (Ag and In or Ga) in this tetragonal lattice breaks the cubic symmetry and introduces anisotropy into the physical properties an essential feature for applications in directional optoelectronics and thermoelectrics [21].

The optimized lattice parameters obtained using the GGA-WC results illustrated in (Table 1), in good agreement with reported experimental and theoretical data. The  $c/a$  ratio in both compounds is approximately 1.98, which is slightly lower than the ideal value of 2.0. This subtle deviation signifies the presence of a minor tetragonal distortion, commonly observed in real chalcopyrite structures. Such a small distortion indicates that the systems maintain a high degree of lattice symmetry and structural integrity, essential for minimizing crystal imperfections, lattice strain, and potential defect states that can trap carriers or act as non-radiative recombination centers.

**Table 1.** Lattice parameters ( $a$ ,  $c$ ) (Å), internal parameter ( $u$ ), bulk modulus  $B$  (GPa), and its pressure derivative  $B'$  for the  $\text{AgGaTe}_2$  and  $\text{AgInTe}_2$  compounds

Compound		$a(\text{\AA})$	$C(\text{\AA})$	$c/a$	$\eta=c/2a$	$U(\text{\AA})$	$B(\text{GPa})$	$B'$
$\text{AgGaTe}_2$	Our Calcul.	6.221	12.558	1.99	1.00	0.250	50.123	5.347
	Exp.	6.288 <sup>a</sup>	11.940 <sup>a</sup>	1.898 <sup>a</sup>	0.949 <sup>a</sup>	-	-	-
		6.283 <sup>b</sup>	11.918 <sup>b</sup>	1.897 <sup>b</sup>	0.948 <sup>b</sup>	0.26 <sup>b</sup>	48.6 <sup>b</sup>	-
$\text{AgInTe}_2$	Our calcul.	6.442	12.925	1.992	0.997	0.231	45.540	5.6122
	Exp.	6.467 <sup>a</sup>	12.633 <sup>a</sup>	1.85 <sup>a</sup>	0.977 <sup>a</sup>	0.262 <sup>a</sup>	-	-

<sup>a</sup>Ref [32], <sup>b</sup>Ref [33]

The variation of Energy as function a volume (Fig. 1). The slight differences in lattice constants and unit cell volumes between  $\text{AgInTe}_2$  and  $\text{AgGaTe}_2$  can be attributed primarily to the difference in covalent radii of the Group III elements. Indium (In), with a covalent radius of 1.56 Å, is significantly larger than gallium (Ga), which has a radius of 1.36 Å. This difference leads to a lattice expansion in  $\text{AgInTe}_2$  along both the  $a$ -axis and  $c$ -axis, resulting in a larger unit cell volume compared to  $\text{AgGaTe}_2$ . This observation is consistent with Vegard's law, which states that the lattice parameters of a solid solution or alloy vary linearly with the atomic radii of the substituting elements. From a materials physics perspective, such atomic substitution not only alters the geometrical framework but also subtly affects bond lengths and bond angles, especially the Ag–Te and In/Ga–Te bonds, which are critical for orbital hybridization and

bandgap formation. For example, a longer In–Te bond in AgInTe<sub>2</sub> leads to weaker orbital overlap compared to the shorter Ga–Te bond in AgGaTe<sub>2</sub>, which can influence both the band dispersion and the effective mass of charge carriers.

Moreover, the bond alternation parameter ( $u$ ) and internal displacement of atoms though not detailed here also play a role in the spatial electron density distribution, anisotropic dielectric response, and polarization effects, which are significant in nonlinear optical applications and in understanding carrier localization phenomena.

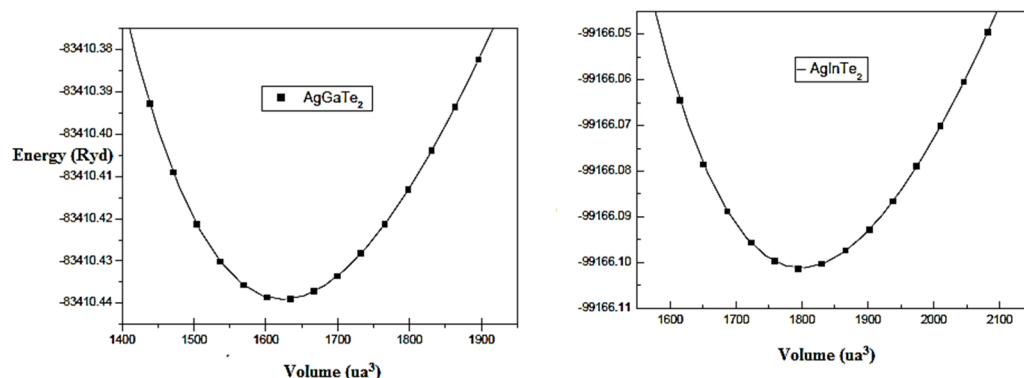


**Figure 1.** The dependence of the total energy on volume was examined for the AgInTe<sub>2</sub> and AgGaTe<sub>2</sub> compounds, aiming to analyze their thermodynamic and structural characteristics

The precision of the computed structural parameters highlights the strength and reliability of the employed computational approach. Although the GGA-WC functional is recognized for its limited accuracy in bandgap predictions, it proves effective in capturing equilibrium structures and volumetric behavior. This consistency in structural modeling provides a dependable foundation for further exploration of the electronic band structure, density of states, and optical characteristics, especially considering that even slight discrepancies in lattice parameters may lead to significant variations in observable physical properties.

In conclusion, both AgInTe<sub>2</sub> and AgGaTe<sub>2</sub> exhibit stable, well-ordered chalcopyrite structures with minimal tetragonal distortion and expected trends in lattice expansion due to atomic substitution. These structural characteristics contribute directly to the favorable semiconducting and optical properties of these materials. Their mechanical stability, structural uniformity, and adaptability to lattice engineering make them strong candidates for advanced applications in photovoltaic energy conversion, infrared photodetection, and thermoelectric energy harvesting.

### 3.2. Electronic Structure Band

The electronic band structure calculations for AgInTe<sub>2</sub> and AgGaTe<sub>2</sub> indicate that both compounds possess a direct bandgap, with the valence band maximum (VBM) and conduction band minimum (CBM) located at the  $\Gamma$ -point in the Brillouin zone (see Figure 2). This direct transition is particularly beneficial for optoelectronic and photovoltaic technologies, as it enables efficient photon absorption and emission without the necessity of phonon involvement. The band structures were derived using the Generalized Gradient Approximation (GGA), based on either prior literature or current computational results (refer to Table 2). These findings align with the well-documented limitation of GGA in underestimating bandgap values due to its inadequate treatment of exchange–correlation interactions. To achieve more reliable electronic gap predictions, the modified Becke–Johnson (mBJ) potential was employed. This semi-local exchange potential significantly improves the description of the electronic structure, resulting in corrected bandgap values of around 0.98 eV for AgInTe<sub>2</sub> and approximately 1.15 eV for AgGaTe<sub>2</sub>. These values are in much closer agreement with available experimental data, confirming that mBJ is more suitable for accurately capturing the quasi-particle bandgap of semiconducting chalcopyrite materials.

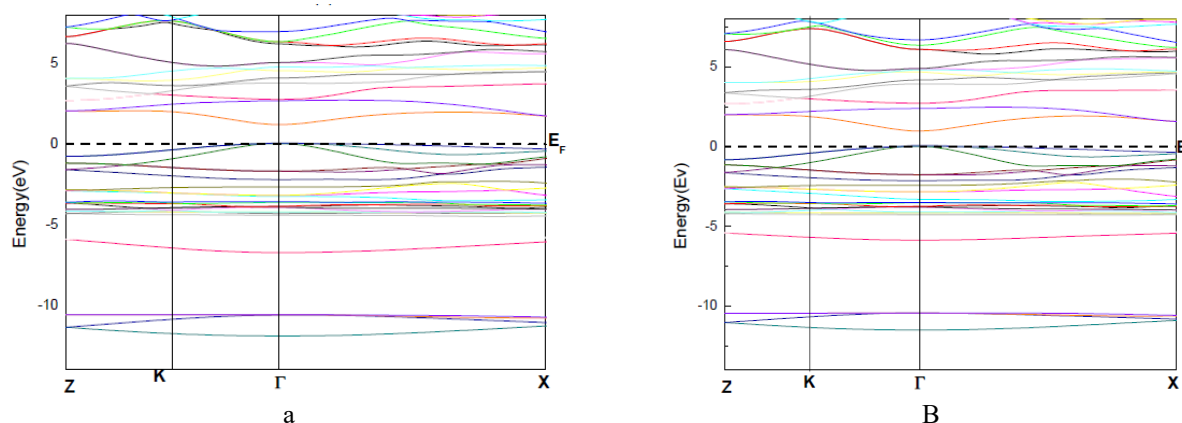


**Figure 2.** Electronic band structures of (a) AgGaTe<sub>2</sub> and (b) AgInTe<sub>2</sub> were computed using the modified Becke–Johnson (mBJ) potential

**Table 2.** Band gap ( $E_g$ ) values of the  $\text{AgInTe}_2$  and  $\text{AgGaTe}_2$  compounds.

E <sub>g</sub> (eV)				
	Our Calcul.		Exp.	Other calcul.
	WC-GGA	mBj		
AgGaTe <sub>2</sub>	0.5	1.18	1.1 <sup>a</sup> , 1.36 <sup>b</sup> , 1.32 <sup>c</sup> 0.93-0.96 <sup>a</sup> , 1.04 <sup>b</sup>	1.10 <sup>a</sup> , 1.21 <sup>b</sup> 1.09 <sup>b</sup>
AgInTe <sub>2</sub>	0.04	1.01		

<sup>a</sup>Ref [32], <sup>b</sup>Ref [33]

In terms of orbital character, the valence band region in both compounds is predominantly composed of Te-5p states, which are strongly hybridized with Ag-4d orbitals. This p–d hybridization plays a vital role in shaping the upper valence bands, leading to relatively flat band dispersion near the VBM and contributing to the high hole effective mass. The conduction band edge, however, exhibits material-specific characteristics: in  $\text{AgInTe}_2$ , the CBM is largely formed by In-5p orbitals, while in  $\text{AgGaTe}_2$ , it consists mainly of Ga-4p states. Due to the smaller and more localized nature of Ga-4p orbitals compared to In-5p, the conduction band in  $\text{AgGaTe}_2$  is slightly more dispersive, which can contribute to a lower electron effective mass and potentially better n-type transport behavior.

The separation between the valence and conduction bands defines the electronic bandgap, and the precise alignment and nature of these bands are crucial in determining the absorption edge, carrier recombination dynamics, and overall efficiency of optoelectronic devices. The clear direct bandgap at the  $\Gamma$ -point and the dominant p–d and p–p interactions in both materials are consistent with what is expected in chalcopyrite semiconductors and support their use as light-absorbing layers in thin-film solar cells, infrared sensors, and photoelectronic modulators.

In summary, the electronic structure analysis demonstrates that  $\text{AgInTe}_2$  and  $\text{AgGaTe}_2$  are both direct gap semiconductors with bandgaps suitable for infrared and near-infrared applications. The mBJ correction effectively mitigates the bandgap underestimation typical of GGA, and the detailed orbital analysis highlights the significant role of Te–Ag hybridization and Group III p-orbitals in shaping the band structure. These characteristics reinforce the potential of these compounds for integration into next-generation optoelectronic and photovoltaic technologies.

### 3.3 Optical Properties

The optical response of  $\text{AgInTe}_2$  and  $\text{AgGaTe}_2$  was investigated through first-principles calculations of the complex dielectric function, expressed as  $\epsilon(\omega) = \epsilon_1(\omega) + i\epsilon_2(\omega)$ , [31] where  $\epsilon_1(\omega)$  represents the real part (describing dispersion) and  $\epsilon_2(\omega)$  the imaginary part (related to absorption). From these fundamental optical quantities, additional key parameters such as the refractive index ( $n$ ), absorption coefficient ( $\alpha$ ), and reflectivity ( $R$ ) were derived, providing a comprehensive view of the materials' interaction with electromagnetic radiation.

The static dielectric constants  $\epsilon_1(0)$  were found to be approximately 12.6 for  $\text{AgGaTe}_2$  and 13.1 for  $\text{AgInTe}_2$ , indicating strong polarization response at zero photon energy. These high values suggest significant electronic polarizability, which is favorable for materials intended for nonlinear optical or capacitive applications. Similarly, the static refractive index  $n(0)$  shows high values of  $\sim 3.55$  for  $\text{AgGaTe}_2$  and  $\sim 3.60$  for  $\text{AgInTe}_2$ , (**Figure 3**) indicating that both compounds are optically dense. Such high refractive indices imply efficient light confinement, which is crucial for enhancing the optical path length in thin-film solar cell structures and improving light absorption efficiency. (**Table 3**).

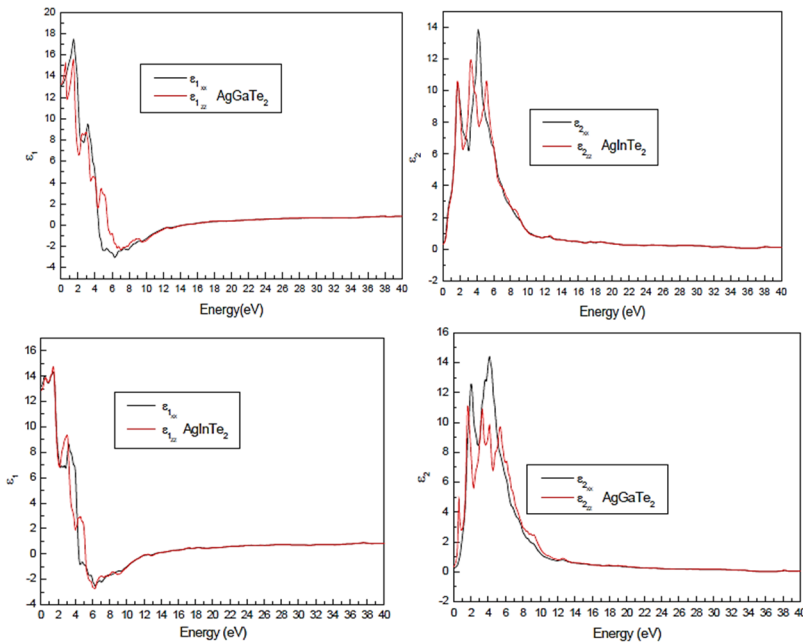


**Figure 3.** The energy-dependent behavior of both the real and imaginary components of the electronic dielectric function  $\epsilon(\omega)$  was analyzed for  $\text{AgGaTe}_2$  and  $\text{AgInTe}_2$  compounds

**Table 3.** Static Dielectric Function ( $\epsilon_1(0)$ ) and Static Refractive Index ( $n(0)$ ) Calculations for AgInTe<sub>2</sub> and AgGaTe<sub>2</sub> Compounds.

	$n(0)$		$\epsilon_1(0)$	
	Our Calcul. WC-GGA	Other calcul. Ref.	Our Calcul.	Other calcul. Ref.
AgInTe <sub>2</sub>	Xx: 3.591 Zz:3.623	Xx: 2.756 Zz: 2.775	Xx:12.942 Zz: 13.193	- -
AgGaTe <sub>2</sub>	Xx: 3.631 Zz: 3.513	Xx: 2.891 Zz: 2.466	Xx: 13.193 Zz: 13.103	Xx: 12.72 Zz: 12.90

Ref [32,33]

The analysis of the imaginary component of the dielectric function,  $\epsilon_2(\omega)$ , indicates that the principal absorption peaks are located at approximately 4.1 eV for AgGaTe<sub>2</sub> and 3.9 eV for AgInTe<sub>2</sub>. These prominent features are attributed to strong interband transitions, notably from Te-5p and Ag-4d states in the valence band to conduction band states largely comprised of Ga-4p or In-5p orbitals. Moreover, the computed absorption coefficient  $\alpha(\omega)$  (as shown in Figure 4) surpasses  $10^5 \text{ cm}^{-1}$  within the visible and near-infrared regions, highlighting the materials' pronounced interaction with light. This high absorption performance is particularly advantageous for photovoltaic applications, as it facilitates efficient solar energy capture even in devices employing ultrathin active layers.

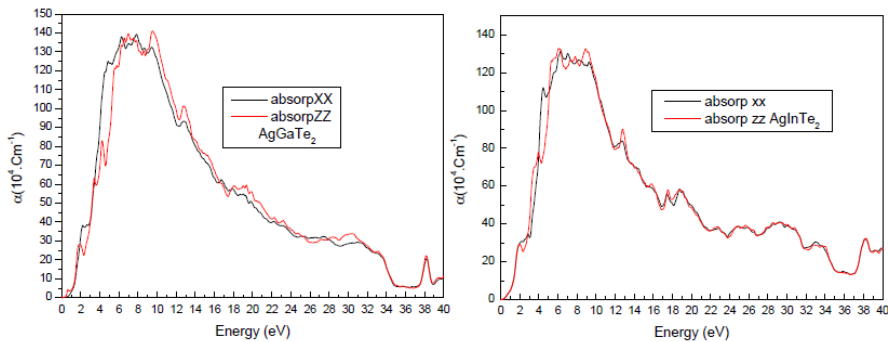


**Figure 4.** The energy-dependent optical conductivity of AgInTe<sub>2</sub> and AgGaTe<sub>2</sub> compounds was examined to assess their electromagnetic response characteristics

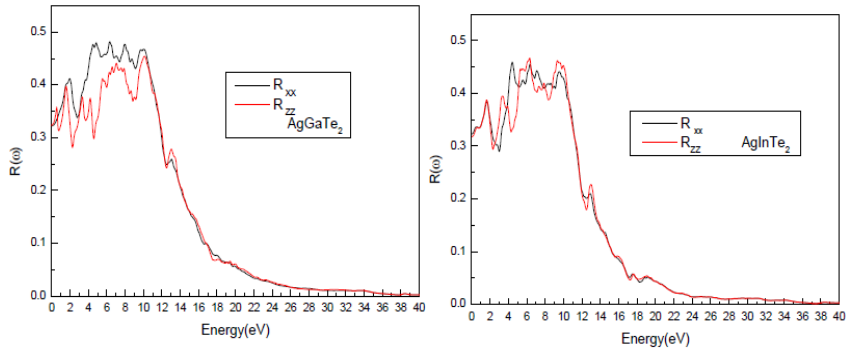


**Figure 5.** The photon energy dependence of the optical reflectivity  $R(\omega)$  was investigated for the AgInTe<sub>2</sub> and AgGaTe<sub>2</sub> compounds to understand their reflective behavior across different spectral regions

The reflectivity spectra demonstrate that both AgInTe<sub>2</sub> and AgGaTe<sub>2</sub> compounds display moderate reflectance approximately 45% in the ultraviolet (UV) region, followed by a gradual decline as the wavelength extends into the visible and infrared ranges. This behavior, characterized by efficient absorption in the visible spectrum alongside partial UV reflectivity (See Figure5), suggests these materials are well-suited for multifunctional optical coatings. In particular, their UV-reflective properties can enhance device longevity and serve as effective radiation filters, making them valuable in optoelectronic and protective applications.

The variation of the refractive index  $n(\omega)$  and the extinction coefficient  $k(\omega)$  as a function of energy is presented in Figure 6. According to the refractive index spectrum, we observe anisotropic behavior, characterized by  $\Delta n(0) = 0.05$  and  $0.02$  for AgInTe<sub>2</sub> and AgGaTe<sub>2</sub>, respectively. The refractive index increases with energy until it reaches a maximum value in the visible region for both compounds. Beyond these energies 1.542 eV for AgInTe<sub>2</sub> and 1.589 eV for AgGaTe<sub>2</sub> it decreases. It is also noted that the peaks shift towards lower energies when moving from Ga to In.

The extinction coefficient  $k(\omega)$  is related to the damping of the oscillation amplitude of the incident electric field. The maximum peak in the extinction coefficient curve appears at the energy value (2.771 eV for AgGaTe<sub>2</sub> and 2.489 eV for AgInTe<sub>2</sub>) where the real part of the dielectric function crosses zero. This is clearly verified for both compounds. Subsequently, the extinction coefficient  $k(\omega)$  decreases with increasing incident photon energy.

Optical conductivity plays a crucial role in evaluating photoelectric conversion efficiency, as it reflects the material's response under illumination. Figure (7) illustrates the energy-dependent optical conductivity profiles of AgGaTe<sub>2</sub> and



AgInTe<sub>2</sub>. Notably, both compounds demonstrate substantial conductivity within the visible spectrum (1.64–3.12 eV), highlighting their suitability for solar energy applications.

Overall, the optical analysis confirms that AgInTe<sub>2</sub> and AgGaTe<sub>2</sub> exhibit highly favorable properties – such as elevated refractive indices, robust absorption across the visible to near-infrared range, and moderate reflectivity in the ultraviolet. These characteristics render them excellent candidates for cutting-edge technologies, including thin-film photovoltaic cells, IR photodetectors, and nonlinear optical components. Furthermore, their capacity to achieve efficient light absorption while maintaining selective transparency enhances their potential integration into advanced multilayer optoelectronic and photonic architectures.

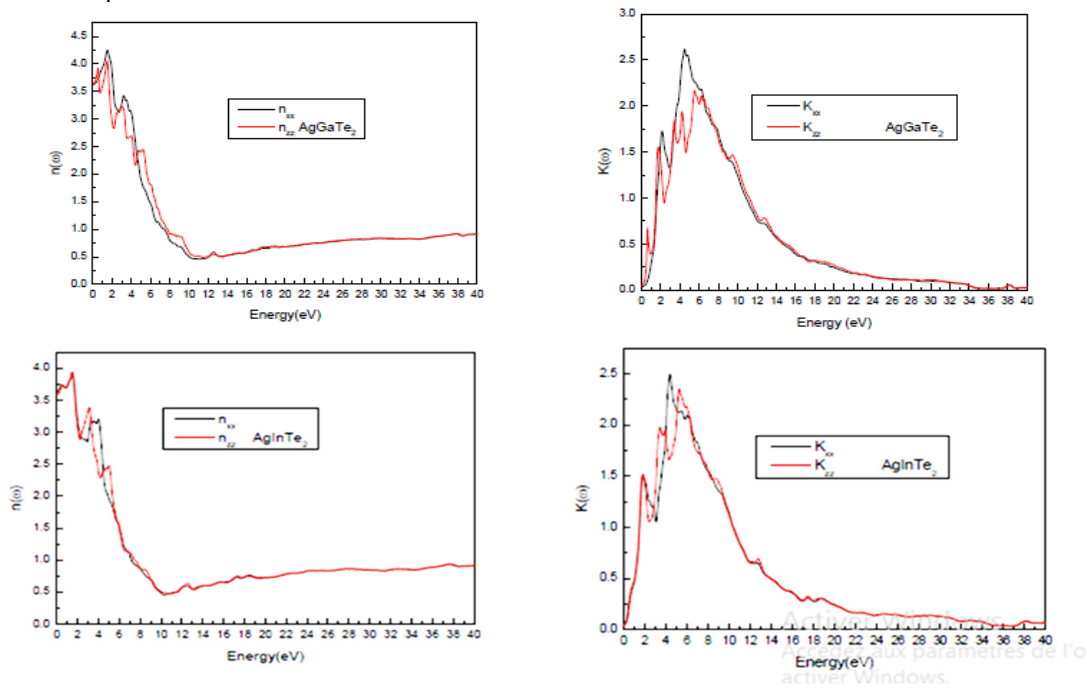


**Figure 6.** Optical Behavior of AgInTe<sub>2</sub> and AgGaTe<sub>2</sub>: Spectral Variation of  $n(\omega)$  and extinction  $k(\omega)$

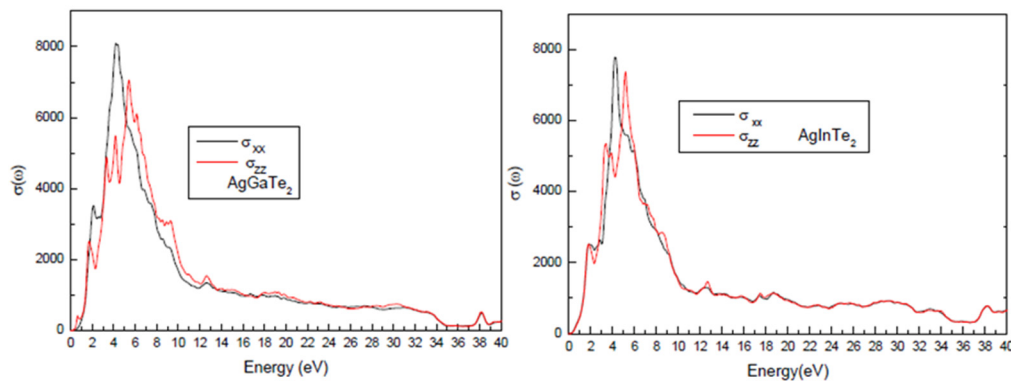


**Figure 7.** The variation in optical conductivity with photon energy was explored for AgInTe<sub>2</sub> and AgGaTe<sub>2</sub> compounds to assess their light-induced electronic response characteristics

## 5. CONCLUSIONS

In this study, we conducted a comprehensive theoretical investigation of the chalcopyrite-type semiconductors AgGaTe<sub>2</sub> and AgInTe<sub>2</sub> using the Full-Potential Linearized Augmented Plane Wave (FPLAPW) method as implemented in the WIEN2k code. Our first-principles calculations provided detailed insights into the structural, electronic, and optical properties of these compounds.

- The optimized lattice parameters are in excellent agreement with available experimental data, confirming the reliability of the computational approach based on the GGA-PBE functional.
- Band structure calculations using the mBJ potential reveal that both materials possess direct bandgaps of approximately 1 eV, which is ideal for optoelectronic and infrared applications.
- The optical analysis demonstrates strong absorption in the visible and near-infrared regions, high static refractive indices, and robust dielectric responses, all of which are critical for efficient light harvesting and photonic functionality.

These findings highlight the potential of AgGaTe<sub>2</sub> and AgInTe<sub>2</sub> as promising candidates for next-generation photovoltaic devices, infrared detectors, and nonlinear optical systems.

## 6. OUTLOOK AND FUTURE DIRECTIONS

To further advance the understanding and technological potential of these materials, future studies may focus on:

- Defect engineering, including the investigation of vacancies, substitutional dopants, or antisite defects, to tailor electronic and optical behavior.
- Alloying strategies, such as partial substitution of Ga, Sb, or Se, to tune the bandgap and optimize performance for specific applications.
- Inclusion of many-body effects, through GW approximation and Bethe–Salpeter Equation (BSE) methods, to more accurately describe excitonic interactions and optical spectra.
- Evaluation of thermal conductivity and carrier mobility, which are crucial for thermoelectric applications and overall device efficiency.

This work lays a strong theoretical foundation for the practical development of Ag-based ternary tellurides and opens avenues for their integration into high-performance optoelectronic and energy conversion technologies.

## ORCID

✉Mosbah Laouamer, <https://orcid.org/0000-0002-6374-6075>; ✉Yamina Benkrima, <https://orcid.org/0000-0001-8005-4065>  
 ✉Redha Meneceur, <https://orcid.org/0000-0002-1801-0835>; ✉Yousra Megdoud, <https://orcid.org/0000-0001-8999-8134>

## REFERENCES

- [1] A.S. Verma, *Philos. Mag.* **89**, 183 (2009). <https://doi.org/10.1080/14786430802593814>
- [2] C. Catella, and D. Burlage, *Mater. Res. Bull.* **23**, 28 (1998). <https://doi.org/10.1557/S0883769400029055>
- [3] M.C. Ohmer, J.T. Goldstein, D.E. Zelmon, A. Waxler, S.M. Hegde, J.D. Wolf, P.G. Schunemann, and T.M. Pollak, *J. Appl. Phys.* **86**, 94 (1999). <https://doi.org/10.1063/1.370704>
- [4] A.S. Verma, and S.R. Bhardwaj, *Phys. Scr.* **79**, 015302 (2009). <https://doi.org/10.1088/0031-8949/79/01/015302>
- [5] V.V. Badikov, O.N. Pivovarov, Y.V. Skokov, O.V. Skrebneva, and N.K. Trotsenko, *Sov. J. Quantum Electron.* **5**, 3502 (1975). <https://doi.org/10.1070/qe1975v005n03abeh011027>
- [6] T. Plirdpring, K. Kurosaki, A. Kosuga, T. Day, S. Firdosy, V. Ravi, G.J. Snyder, *et al.*, *Adv. Mater.* **24**, 3622 (2012). <https://doi.org/10.1002/adma.201200732>
- [7] T. Plirdpring, K. Kurosaki, A. Kosuga, M. Ishimaru, A. Harnwunggmoung, T. Sugahara, Y. Ohishi, *et al.* *Mater. Trans.* **53**, 1212 (2012). <https://doi.org/10.2320/matertrans.e-m2012810>
- [8] R. Liu, L. Xi, H. Liu, X. Shi, W. Zhang, and L. Chen, *Chem. Commun. (Camb.)* **48**, 3818 (2012). <https://doi.org/10.1039/C2CC30318C>
- [9] J. Yao, N. Takas, M. Schlieft, D. Paprocki, P. Blanchard, H. Gou, A. Mar, *et al.* *J. Aitken, Phys. Rev. B*, **84**, 075203 (2011). <https://doi.org/10.1103/PhysRevB.84.075203>
- [10] Y. Li, Q. Meng, Y. Deng, H. Zhou, Y. Gao, Y. Li, J. Yang, and J. Cui, *Appl. Phys. Lett.* **100**, 231903 (2012). <https://doi.org/10.1063/1.4726109>
- [11] A. Kosuga, T. Plirdpring, R. Higashine, M. Matsuzawa, K. Kurosaki, and S. Yamanaka, *Appl. Phys. Lett.* **100**, 042108 (2012). <https://doi.org/10.1063/1.3678044>
- [12] A.V. Kopytov, and A.V. Kosobutsky, *Phys. Solid State*, **52**, 1359 (2010). <https://doi.org/10.1134/s1063783410070061>
- [13] D. Xue, K. Betzler, and H. Hesse, *Phys. Rev. B*, **62**, 13546 (2000). <https://doi.org/10.1103/physrevb.62.13546>
- [14] A.H. Reshak, *Physica B*, **369**, 243 (2005). <https://doi.org/10.1016/j.physb.2005.08.038>
- [15] S. Sharma, A.S. Verma, and V.K. Jindal, *Mater. Res. Bull.* **53**, 218 (2014). <https://doi.org/10.1016/j.materresbull.2014.02.021>
- [16] E. Wimmer, “Computational methods for atomistic simulations of materials,” *Materials Science and Engineering: B*, **37**(1-3), 72 (1996). [https://doi.org/10.1016/0921-5107\(95\)01459-4](https://doi.org/10.1016/0921-5107(95)01459-4)
- [17] P. Kiréev, *la physique des semi-conducteur*, (Mir, Moscow, 1979).
- [18] M. Born, j., and R. Oppenheimer, *Ann. Phys.* **87**, 457 (1927). <https://doi.org/10.1002/andp.19273892002>
- [19] D.R. Hartree, *Mathematical Proceedings of the Cambridge Philosophical Society*, **24**(1), 89 (1928). <https://doi.org/10.1017/S0305004100011919>
- [20] V. Fock, *Z. Phys.* **61**, 126 (1930). <http://dx.doi.org/10.1007/BF01340294>
- [21] A. Zunger, and A.J. Freeman, *Phys. Rev. B*, **16**, 2901 (1977). <https://doi.org/10.1103/PhysRevB.16.2901>
- [22] J.P. Perdew, and A. Zunger, *Phys. Rev. B*, **23**, 5048 (1981). <https://doi.org/10.1103/physrevb.23.5048>
- [23] L.H. Thomas, “The calculation of atomic fields,” *Mathematical Proceedings of the Cambridge Philosophical Society*, **23**(5), 542 (1927). Published online by Cambridge University Press: 24 October 2008. <https://doi.org/10.1017/S0305004100011683>
- [24] E. Fermi, *Z. Phys.* **48**, 73 (1928). <https://doi.org/10.1007/bf01351576>
- [25] P. Hohenberg, and W. Kohn, *Phys. Rev.* **136**, B864 (1964). <https://doi.org/10.1103/PhysRev.136.B864>
- [26] J.P. Perdew, and Y. Wang, *Phys. Rev. B*, **45**, 13244 (1992). <https://doi.org/10.1103/physrevb.45.13244>
- [27] A. Chahed, O. Benhelal, H. Rozale, S. Laksari, and N. Abbouni, *Phys. Status Solidi, B*, **244**, 629 (2007). <https://doi.org/10.1002/pssb.200642050>
- [28] S. Ullah, U.D. Haleem, G. Murtaza, T. Ouahrani, R. Khenata, S. Naeemullah, Bin Omran, *J. Alloys Compd.* **617**, 575 (2014). <https://doi.org/10.1016/j.jallcom.2014.08.058>
- [29] E. Jaffe, A. Zunger, *Phys. Rev. B*, **29**, 1882 (1983). <https://doi.org/10.1103/PhysRevB.29.1882>
- [30] J.L. Shay, and J.H. Wernick, *Ternary Chalcopyrite Semiconductors: Growth, Electronic Properties and Applications*, (Pergamon Press, Oxford, 1975). <https://doi.org/10.1016/C2013-0-02602-3>

- [31] W.N. Honeyman, K.H. Wilkinson, J. Phys. D, **4**, 1182 (1971). <https://doi.org/10.1088/0022-3727/4/8/319>
- [32] K. Beggas, et al., Indian J. Phys. **98**, 2755 (2024). <http://dx.doi.org/10.1007/s12648-023-03049-4>
- [33] S.A. Bendehiba, et al. Materials Science in Semiconductor Processing, **183**, 108772 (2024), <https://doi.org/10.1016/j.mssp.2024.108772>

**ПОКРАЩЕНЕ ДОСЛІДЖЕННЯ НАПІВПРОВІДНИКІВ ХАЛЬКОПРИТУ  $\text{AgGaTe}_2$  ТА  $\text{AgInTe}_2$  НА ОСНОВІ ПЕРШОПРИНЦИПІВ ЗА ДОПОМОГОЮ FPLAPW В РАМКАХ WIEN2K: СТРУКТУРНІ, ЕЛЕКТРОННІ ТА ОПТИЧНІ ВЛАСТИВОСТІ**

**Абдельгані Кубіл<sup>1</sup>, Мохамед Хеттал<sup>1</sup>, Юсра Мегдуд<sup>1</sup>, Мосбах Лауамер<sup>2</sup>, Яміна Бенкрима<sup>3</sup>, Латіфа Тайрі<sup>4</sup>, Редха Менесер<sup>2</sup>**

<sup>1</sup>Інститут наук, Університетський центр Тіпаза, Алжир

<sup>2</sup>Підрозділ UDERZA, Технологічний факультет, Університет Ель-Уед 3900, Алжир

<sup>3</sup>Вища нормальна школа Уаргла 3000 Алжир

<sup>4</sup>Дослідницький центр промислових технологій CRTI, Р.О. Скринька 64, Cheraga16014 Алжир, Алжир

У цій статті ми представляємо детальне теоретичне дослідження потрібних халькопіритових напівпровідників  $\text{AgGaTe}_2$  та  $\text{AgInTe}_2$  з використанням розрахунків з перших принципів, заснованих на теорії функціоналу густини (DFT). Моделювання проводиться в рамках формалізму повнопотенціальної лінеаризованої доповненої плоскої хвилі (FPLAPW), реалізованого в обчислювальному пакеті WIEN2k. Структурні властивості оптимізовані за допомогою функціоналу обміну-кореляції WC-GGA, тоді як електронні та оптичні відгуки уточнюються за допомогою модифікованого потенціалу Бекке-Джонсона (mBJ), відомого своєю покращеною точністю оцінки ширини забороненої зони. Дослідження включає ретельну оцінку електронних зонних структур та різних оптичних параметрів, включаючи комплексну діелектричну функцію, коефіцієнт поглинання, показник заломлення, функцію втрат енергії та відбивну здатність. Результати показують, що обидва матеріали мають прямі заборонені зони, які знаходяться в оптимальному діапазоні для поглинання сонячними елементами. Крім того, ці сполуки демонструють сильне поглинання світла у видимому та ближньому інфрачервоному діапазонах, високі показники заломлення та помітні міжзонні переходи. Такі особливості підкреслюють їхню придатність для фотоелектричних технологій, особливо в тонкоплівкових конфігураціях, де покращене захоплення світла та генерація носіїв заряду є критично важливими. Більше того, спостережувані оптичні та електронні властивості також вказують на можливе використання в інфрачервоному детектуванні та нелінійних оптоелектронних системах. Загалом, результати надають цінне теоретичне розуміння оптоелектронних характеристик телуридних халькопіритів на основі срібла, підкреслюючи їхній потенціал як екологічно чистих та ефективних матеріалів для майбутніх рішень у сфері сонячної енергетики.

**Ключові слова:** FPLAPW; теорія функціоналу густини; модифікований аналіз Бекке-Джонсона; електронна структура; оптичний аналіз